INTERNATIONAL JOURNAL OF CIRCUITS, SYSTEMS AND SIGNAL PROCESSING
DOI: 10.46300/9106.2022.16.138 Volume 16, 2022

Compression of Hyper Spectral Images using Tensor Decomposition Methods

B. Sucharitha[1], Dr. K. Anitha Sheela[2]
Electronics and Communication Engineering Department,
Jawaharlal Nehru Technological University Hyderabad
Kukatpally, Hyderabad,
India.

Received: May 24, 2022. Revised: August 15, 2022. Accepted: September 17, 2022. Published: October 7, 2022.

Abstract: - Tensor decomposition methods have beenrecently identified as an effective approach for compressing high-dimensional data. Tensors have a wide range of applications in numerical linear algebra, chemo metrics, data mining, signal processing, statics, and data mining and machine learning. Due to the huge amount of information that the hyper spectral images carry, they require more memory to store, process and send. We need to compress the hyper spectral images in order to reduce storage and processing costs. Tensor decomposition techniques can be used to compress the hyper spectral data. The primary objective of this work is to utilize tensor decomposition methods to compress the hyper spectral images. This paper explores three types of tensor decompositions: Tucker Decomposition (TD_ALS), CANDECOMP/PARAFAC (CP) and Tucker_HOSVD (Higher order singular value Decomposition) and comparison of these methods experimented on two real hyper spectral images: the Salinas image (512 x 217 x 224) and Indian Pines corrected (145 x 145 x 200). The PSNR and SSIM are used to evaluate how well these techniques work. When compared to the iterative approximation methods employed in the CP and Tucker_ALS methods, the Tucker_HOSVD method decomposes the hyper spectral
image into core and component matrices more quickly. According to experimental analysis, Tucker HOSVD's reconstruction of the image preserves image quality while having a higher compression ratio than the other two techniques.

Keywords:-Hyper Spectral Image, Tensor, Tensor Decomposition, PSNR, SSIM.

I. INTRODUCTION

Hyper spectral (HS) image compression has drawn a lot of interest due to the massive amount of data that was gathered by the spectrometers, which consists of hundreds of non-overlapping spectral bands with extremely high inter-band spectral correlation. HS images are used in a variety of applications, such as locating and tracking soldiers during military operations [1], monitoring quality in the agricultural sector [2], finding and tracking parts in the manufacturing industry [3], tracking and tracing celestial bodies in space, examining the Earth's surface for classifying minerals, and tracking in remote sensing, as well as locating and tracking natural disasters like floods and droughts [4].

HS-imaginary captures the information or scene at different wave lengths across the electro-magnetic spectrum from 400 to 2500 nm, which is outside the range of human vision. Each pixel consists of a spectrum corresponding to various wavelengths. The fundamental goal of HS imaging is to extract the pixel spectrum from a scene image. Each image pixel is made up of hundreds of values that correspond to the sampling of the pixel's continuous spectrum [5]. HS imagery is more accurate and detailed than other types of sensed data. The HS image means a large number of images captured at different wavelengths. The image is acquired at a certain spectral band, or wavelength range, of the electromagnetic spectrum, and the HS image changes color at different wavelengths. The HS image is defined in the form of a data cube (K, L, and M), where K and L indicate the spatial dimensions and M indicates the spectral dimension.

HSI compression provides challenges in HS image processing, necessitating HSI storage and transmission

bandwidth. For instance, the 512 x 512 x 224, 16 bit AVIRIS - Airborne Visible/Infrared Imaging Spectrometer dataset requires Giga Bytes of memory storage. HS image compression is a technique for reducing an image's size without compromising its quality. The cost of the bandwidth and storage on the device is decreased by HS image compression. HS Image Compression is primarily divided into two categories: Lossless Compression [6] and Loss Compression. The foundation of HS image compression is divided into 2 categories: transformed-based techniques like DWT (Discrete Wavelet Transform), DCT (Discrete Cosine Transform), and decomposition techniques like tensor decomposition, SVD, and PCA.

The transform-based technique is the most widely used 2D compression method, which has been extended to 3Dimages. It applies a transformation function to the image's three dimensions, transforming theimage pixels'grey values into the frequency domain. For compressing HS images, transform-based techniques like discrete flourier transform,discrete cosine transform, discrete wavelet and karhunene-loeve transform are commonly used. These transform-based techniques can be applied with other methods like predictive, compressive sensing, tensor decomposition (TD), etc. Tensor decomposition methods are the most current techniques for HS image compression that outperform traditional transform-based methods.H.Wang et al. [7] proposed a method that uses Principle Component Analysis (PCA) in JPEG 2000 for decorrelation of the spectrum. Fowler et al. [8] proposed a low-complexity PCA which is spatially sampled. Karami et al. [9] proposed 3D-DCT method is applied to the HS image. It converts pixels into low and high energy frequency coefficients using DCT. Low frequencyenergy coefficients are dropped by quantization, and TD is applied to high frequencyenergy coefficients to create a compressed image. Karami et al. [10] proposed 3D-DWT in conjunction with Tucker decomposition, which uses DWT to divide an image into four subgroups: LLLH, HL, and HH band. Tucker decomposition is applied to these four groups and finally a coder to the core tensor to create a compressed image. A reverse process is applied to reconstruct the original image. Wang et al. [11] proposed a method which used 3-DWT to separate high and low frequency regions. To create a compressed image, Turbo channel coding is used for higher frequency regions and 3D-SPIHT (set partitioning in hierarchical trees) for low frequency regions to create a compressed image. Cheng et al. [12] proposed the EZW (Embedded Zero tree Wavelet) algorithm. EZW is a hybrid method of an integer KLT and an integer DWT, which provides higher efficiency and a higher compression ratio compared to existing methods. A genetic algorithm has been proposed by Karami et al. [13] which is named Particle Swarm Optimization Non-negative Tuckerdecomposition (NTD). A genetic algorithm is used to obtain a final optimized solution after implementing NTD. Rajesh and Gagan Kumar [14] proposed two implementations of the image compression algorithm, and Fangl, He [15] proposed a CP compression technique which decomposes the given tensor image into rank-1 tensors. Tensor decomposition techniques can achieve high compression ratios with good PSNR, less computing cost and higher accuracy when compared to transform-based techniques.Dimensionality Reduction for Classification Methods Using Tensor Modeling was proposed by N. Renard and S. Bourennane [16]. The dimensions were reduced by using a PCA joint and an orthogonal projection onto a lower subspace dimension of the spatial way.HYDICE data from the real world are used in the experiment. The use of dimension reduction increased the hyper spectral image classifier's effectiveness.In this paper three Tensor decomposition methods have used to compress the two real HS images. Tensor decomposition methods remove the spectral and spatial redundancy exists in HS image.

The paper is organized as: Section II deals with the fundamental concept of tensors and their operations. Section III deals with three main tensor decomposition methods Section IV examines and draws conclusions from the experimental results.Section V of the study finishes with a list of potential future work.

II. INTRODUCTION TO TENSORS

Tensors are commonly utilized in a variety of applications, including machine learning, data analytics and so on. Tensors are generalizations of matrices to higher dimensions.Higher order tensors are used as a mathematical representation of images. A tensor Tis an M - Dimensional (Multi- Dimensional) array of order N. It is acomponent of the product of M Vector space.
$T \in \mathbb{R}^{K X L X M}$. The order or modes of the tensor are indicated by dimensionality. A vector is a 1st order Tensor, a matrix is a 2nd order Tensor, and three or higher orders are known as Tensors [17]. Fig 2 shows the visualization of tensors of order - 0, 1, 2, and 3.As HS images have three dimensions (Rows, Cols, and Channel), they are represented as a 3rdorder Tensor in Fig 2.T_{KLM} represents an element (K, L and M) of a 3rd order Tensor T.

Fig 1: Vector, Matrix and Tensor

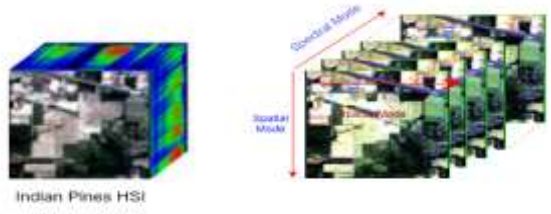

Fig 2: HS Image Cube

A. Fiber: -Fibers are the matrix's higher order Rows and Columns, specified by a single index. A matrix column is a mode-1 fiber. A matrix row is represented by the Mode-2. Similar to this, 3rd order tensors have three fibers: row, column, and tube, which are denoted by the letters $T_{:lm}$,$T_{k:m}$, and $T_{kl:}$ correspondingly as shown in Fig3.

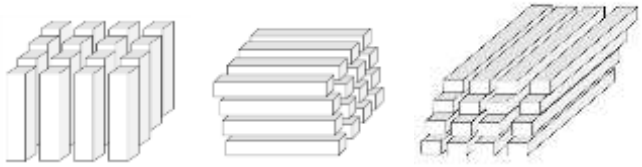

Fig 3: Column Fiber, Row Fiber and Tube Fiber

B. Slices:- By fixing all but two indices, two-dimensional Sections of a tensor are defined as Slices.The horizontal, lateral and frontal slices are shown in Fig 4.

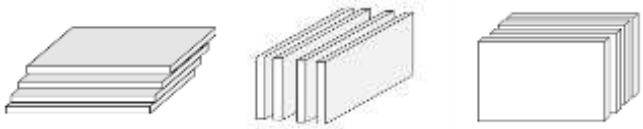

Fig 4: Horizontal slices, Lateral and Frontal slices

C. Rank-1 Tensor: -A multidimensional tensor is strictly considered to be of rank - 1 if it can be reduced to the outer product of M vectors. A rank-1 matrix can be represented as T= aob and rank-1 third order tensor can be represented asT= ao b o c.Fig 5 represents the rank-1 concept graphically.

D. Tensor Rank:-The Rank of a tensor(T) is the lowest number of rank-1 tensors necessary to produce T as their sum. A rank-R third order tensor can be written as

$$T = \sum_{r=1}^{R} \lambda_r \, a_r o \, b_r o \, c_r = [\![\lambda : A, B, C]\!]$$

The A,B,C are called the factor matrices and λris frequently employed to absorb the corresponding weights during the normalization of the column of the factor matrices.

The Norm of a 3rd order tensor $T \in \mathbb{R}^{K \times L \times M}$is given by

$$\|T\| = \sqrt{\sum_{k=1}^{K} \sum_{l=1}^{L} \sum_{m=1}^{M} T_{klm}^2}$$

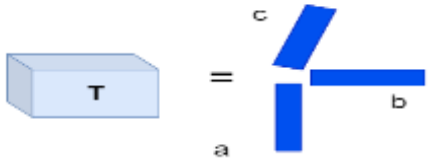

Fig 5: Rank-1 3rd order Tensor

E. Inner Product:-The inner product of 3rd order tensors $S,T \in \mathbb{R}^{K \times L \times M}$ is given by

$$\langle S, T \rangle = \sqrt{\sum_{k=1}^{K} \sum_{l=1}^{L} \sum_{m=1}^{M} S_{klm} \, T_{klm}}$$

The outer product of the third order tensor is represented as T = a(1) o a(2) o....o a(M) with

$$t_{i_1 i_2 \ldots\ldots i_N} = a_{i_1}^{(1)} a_{i_2}^{(2)} \ldots\ldots a_{M}^{(M)}$$

F. Matricization:- Rearranging the elements of a tensor into a matrix is called Unfolding.For instance 3 x 4 x 2 tensor can be arranged as a 2 x 12 matrix or a 3 x 8 and so on. Let the frontal slices of $T \in \mathbb{R}^{3 \times 4 \times 2}$ be

$$\boldsymbol{T}_1 = \begin{bmatrix} 1 & 2 & 3 & 4 \\ 4 & 6 & 8 & 6 \\ 3 & 6 & 9 & 7 \end{bmatrix}, \quad \boldsymbol{T}_2 = \begin{bmatrix} 3 & 2 & 3 & 8 \\ 1 & 7 & 9 & 3 \\ 8 & 2 & 8 & 5 \end{bmatrix}$$

Then, the 3 mode-n unfolding are

$$\boldsymbol{T}_{(1)} = \begin{bmatrix} 1 & 2 & 3 & 4 & 3 & 2 & 3 & 8 \\ 4 & 6 & 8 & 6 & 1 & 7 & 9 & 3 \\ 3 & 6 & 9 & 7 & 8 & 2 & 8 & 5 \end{bmatrix}, \boldsymbol{T}_{(2)} = \begin{bmatrix} 1 & 4 & 3 & 3 & 1 & 8 \\ 2 & 6 & 6 & 2 & 7 & 2 \\ 3 & 8 & 9 & 3 & 9 & 8 \\ 4 & 6 & 7 & 8 & 3 & 5 \end{bmatrix}$$

$$\boldsymbol{T}_{(3)} = \begin{bmatrix} 1 & 4 & 3 & 2 & 6 & 6 & 3 & 8 & 9 & 4 & 6 & 7 \\ 3 & 1 & 8 & 2 & 7 & 2 & 3 & 9 & 8 & 8 & 3 & 5 \end{bmatrix}$$

G. Tensor Multiplication:-The n- mode (matrix) product of a tensor$\boldsymbol{T} \in \mathbb{R}^{M1 \times M2 \times \ldots\ldots Mn}$with a matrix $U \in \mathbb{R}^{J \times Jn}$ is denoted by ($\boldsymbol{T} x_n \boldsymbol{U}$).

Let Tbe the tensor given below

$$\begin{bmatrix} 1 & 2 & 3 & 4 \\ 4 & 6 & 8 & 6 \\ 3 & 6 & 9 & 7 \end{bmatrix} \begin{bmatrix} 3 & 2 & 3 & 8 \\ 1 & 7 & 9 & 3 \\ 8 & 2 & 8 & 5 \end{bmatrix}$$

and let $U = \begin{bmatrix} 2 & 4 & 6 \\ 3 & 5 & 7 \end{bmatrix}$. Then, the product

$$\boldsymbol{y} = \boldsymbol{T} x_1 \boldsymbol{U} \in \mathbb{R}^{3 \times 4 \times 2}$$

$$Y_1 = \begin{bmatrix} 36 & 64 & 92 & 74 \\ 44 & 78 & 112 & 91 \end{bmatrix},$$
$$Y_2 = \begin{bmatrix} 58 & 44 & 90 & 58 \\ 70 & 55 & 110 & 74 \end{bmatrix}$$

H. Matrix Kronecker Product:- Consider two matrices $A \in \mathbb{R}^{I \times J}$ and $B \in \mathbb{R}^{K \times L}$ then, the Kronecker product is denoted by A ⊗ B and defined by

$$A \otimes B = \begin{bmatrix} a_{11}B & a_{12}B \ldots\ldots a_{1J}B \\ a_{21}B & a_{22}B \ldots\ldots a_{2J}B \\ & . \\ & . \\ a_{I1}B & a_{I2}B \ldots\ldots a_{IJ}B \end{bmatrix} \quad \text{and}$$

the result is a matrix of size (IK) X (JL)

I. Matrix Khatri –Raoproduct: - Consider two matrices A $\in \mathbb{R}^{I \times K}$ and B $\in \mathbb{R}^{J \times K}$ then, the Khatri –Rao product is denoted by A ⊙ B and defined by A⊙ B = [a1⊗b1a2⊗b2 ⋯⋯aK⊗bK] and the result is a matrix of size (IJ) x K. It is the matching column wise Kronecker product and a ⊗ b =a ⊙ b are identical if a and b are vectors .

J. Hadamard product: - It is the element wise product.Consider two matrices A and B are of same size of I x J then Hadamard product is denoted by A * B and defined by

$$A * B = \begin{bmatrix} a_{11}b_{11} a_{12}b_{12} \ldots\ldots a_{1J}b_{1J} \\ a_{21}b_{21} a_{22}b_{22} \ldots\ldots a_{2J}b_{2J} \\ & . \\ & . \\ a_{I1}b_{I1} a_{I2}b_{I2} \ldots\ldots a_{IJ}b_{IJ} \end{bmatrix}$$

III. TENSOR DECOMPOSITIONS METHODS

Tensor decompositions are useful techniques for tensor analysis. These have been the subject of in-depth research in many disciplines including signal processing, psychometrics, neuroscience, communication, machine learning, chemo metrics, biometrics, quantum physics, and quantum chemistry[18]. Several matrix decompositions are generalised by tensor decompositions. The popular tensor decompositions are tensor rank decomposition, higher order singular value Decompositions, Tucker Decomposition (TD), Hierarchical Tucker decompositions, CANDECOMP/PARAFAC (CP) Decomposition and Block term decomposition and are the two most commonly used TD techniques.

A. CANDECOMP/PARAFAC(CP)

Decomposition Method: -By representing the 3D HSI as a 3-way tensor, the canonical decomposition approach[19] is employed to minimize the size of the dataset. As seen in Fig 6, the canonical decomposition method decomposes the given tensor as the addition of rank-1 tensors. In general these images can be visualized as a three-mode Tensor as shown in Fig 2. The HS image, $T \in \mathbb{R}^{K \times L \times M}$, where K, L, and M are the parameters for the height, width, and spectral channel.

The Third order HS image tensor $T \in \mathbb{R}^{K \times L \times M}$ can be written as the sum of Rank- 1 tensor

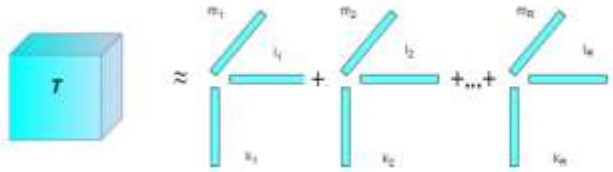

Fig 6: CP decompositions as a three way array

$$\boldsymbol{T} \approx \sum_{r=1}^{R} p_r \; o \; q_r \; o \; N_r$$

Where R is a positive Integer, $p_r \in \mathbb{R}^K$, $q_r \in \mathbb{R}^L$ and $n_r \in \mathbb{R}^M$ for r= 1, 2, 3…..The third order element wise HS image tensor can be written as

$$\boldsymbol{T}_{klm} \approx \sum_{r=1}^{R} p_{kl} \, q_{lm} \, n_{mk}$$

for k=1,2,3…..K, l=1,2,3…..L and m=1,2,3…..M as shown in Fig 6.The combination of the vector from the rank-1component is referred to as factormatrices.The third order HSI tensor may be written in matrix form also

$$\boldsymbol{T}_{(1)} \approx P(N \odot Q)^T \; ; \; \boldsymbol{T}_{(2)} \approx Q(N \odot P)^T;$$

$$\boldsymbol{T}_{(3)} \approx N(Q \odot P)^T \; ;$$

Where ⊙ denotes the Khatri–Rao product and P,Q,N are the Rank-1 Vectors as shown in equation.

$$P = [p_1, p_2, p_3, \ldots\ldots p_R] \; ; \quad Q = [q_1, q_2, q_3, \ldots q_R] \; ;$$

$$N = [n_1, n_2, n_3, \ldots n_r]$$

Finally CP model can be expressed as

$$\boldsymbol{T} \approx [\![P, Q, N]\!] \sum_{r=1}^{R} p_r \circ q_r \circ n_r$$

If P,Q,N are adjusted to unit length with the absorbed weights into the vector$\lambda \in \mathbb{R}^R$

Then $\boldsymbol{T} \approx [\![\lambda ; P, Q, N]\!] = \sum_{r=1}^{R} \lambda_r \, p_r \circ q_r \circ n_r$

CP decomposition with ALS algorithm:-The main problem with CP decomposition is determining how many rank-1 tensors to use. The rank of a tensor cannot be determined by a finite procedure. [20]. The iterative alternate least squares approach is used to calculate the rank of tensors [21-25]. The iterative approach first fixes P and Q to solve N, then fixes P and N to solve Q, then fixes Q and N to solve P, and so on until some convergence criterion is satisfied.

Procedure

Input: HSImage dataset$\boldsymbol{T} \in \mathbb{R}^{K \times L \times M}$
Compression:
Initialize: Set randomly P, Qand N.
Repeat
$P = \boldsymbol{T}_{(1)} (N \odot Q)[N^T N * Q^T Q]^{\dagger}$ and save theNormalization of the columns in P as v,
$Q = \boldsymbol{T}_{(2)} (N \odot P)[Q^{TQ} * P^T P]^{\dagger}$ and save theNormalization of the columns in Q as v,
$N = \boldsymbol{T}_{(1)} (Q \odot P)[Q^T Q * P^T P]^{\dagger}$ and save theNormalization of the columns in P as v.
Until $\| \boldsymbol{T} - \overline{\boldsymbol{T}} \|_F / \| \boldsymbol{T} \|_F < \epsilon$, ϵ is a constant

B. Tucker Decompositions (TD):- Consider a 3D tensor (HS image) $\boldsymbol{T} \in \mathbb{R}^{k \times L \times M}$ decomposed into core and component matrices[26-28] as shown in Fig 7 .

$$\boldsymbol{T} \approx \boldsymbol{G} \times_1 A \times_2 B \times_3 C = \sum_{i=1}^{I1} \sum_{j=1}^{I2} \sum_{l=1}^{I3} g_{pqr} \, a_i \circ b_j \circ c_l = [\![\boldsymbol{G} ; A, B, C]\!]$$

Where $A \in \mathbb{R}^{K \times i1}$, $B \in \mathbb{R}^{L \times i2}$ and $C \in \mathbb{R}^{M \times i3}$ are orthogonal component matrices and $G \in \mathbb{R}^{i1 \times i2 \times i3}$ is called core tensor.Tucker introduced the decomposition of a tensor in 1966. Tucker decomposition using Alterative least square and Tucker decomposition using Higher Order Singular value Decomposition are two well methods used for HS image compression.

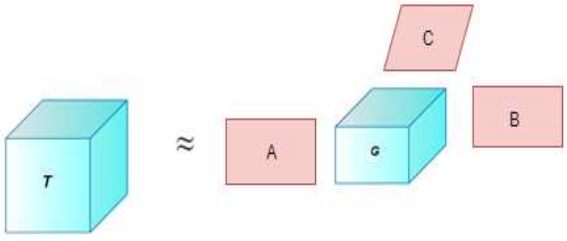

Fig 7 : Tucker Decomposition

B.1 TD Decomposition with ALS algorithm

Tucker Decomposition using ALS approximation algorithm decomposes the given tensor into core tensor and orthogonal component matrices with initial guess. TD decomposition with ALS algorithm is explained in below.

Input : HSImage dataset$\boldsymbol{T} \in \mathbb{R}^{K \times L \times M}$, R Compression

Initialize : Set randomly i1,i2,i3 .

Repeat
$A = \boldsymbol{T}_{(1)} (C \odot B)[C^T C * B^T B]^{\dagger}$ and save theNormalization of the columns in A as v,
$B = \boldsymbol{T}_{(2)} (C \odot A)[B^T B * A^T A]^{\dagger}$ and save theNormalization of the columns in B as v,
$C = \boldsymbol{T}_{(1)} (B \odot A)[B^T B * A^T A]^{\dagger}$ and save theNormalization of the columns in C as v.
Until $\| \boldsymbol{T} - \overline{\boldsymbol{T}} \|_F / \| \boldsymbol{T} \|_F < \epsilon$, ϵ is a constant

B.2 Tucker Decomposition – HOSVD

A straightforward method for solving the Tucker decomposition would be to solve each mode-k metricized form of the Tucker decomposition for A(k). HOSVD can be considered as a generalization of the matrix SVD. The algorithm is shown below.

Procedure TD-HOSVD ($\boldsymbol{T}$,R_1,R_2,R_3):
for k=1,2,3…N do
$R^{(n)} \rightarrow A^{(n)}$left single leading vector of $\boldsymbol{T}_{(N)}$
end for
$\boldsymbol{G} \leftarrow \boldsymbol{T} \times_1 A^{(1)^T} \times_2 A^{(2)^T} \times_3 \ldots \times_N A^{(N)^T}$
Return $\boldsymbol{G}$, $A^{(1)} A^{(2)} \ldots \ldots \ldots A^{(N)}$
End procedure

IV. SIMULATION RESULTS

Experimentation is carried out on two different Hyper Spectral Images: Salinas and IndianPines as shown in Fig 8. Indian Pines was taken by NASA's AVIRIS sensor above Indian Pines, Indiana, and it has 145 by 145 pixels and 224 channels/bands in the wavelength range of 400nm to 2500nm.

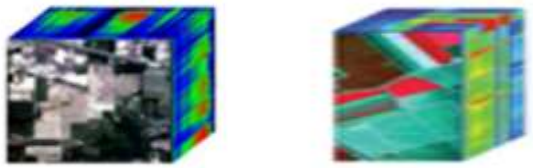

Fig 8 : Indian Pine HS Image Data set and Salinas HS Image

Indian Pines Corrected (145 x145 x200) forms by removing the excessive noise and water absorption bands. The 512 x217 x 224 pixel Salinas scene was captured in the range of 400nm to 860nm over California's Salinas Valley. Salinas HS image of size 512 x 217 x 224 is compressed using three tensor Decompositions methods- CP Decompositions, Tucker Decomposition –HOSVD and Tucker Decomposition – ALS.

Table 1 : PSNRs of Salinas HS image

S.No	BANDS	CP	TD_ALS	TD_HOSVD
1	7	38.40	38.60	38.73
2	28	42.89	46.33	46.54
3	37	43.54	45.73	45.946
4	42	44.35	48.09	48.22
5	60	38.94	43.58	43.70
6	98	35.50	37.56	37.71
7	170	29.22	29.06	29.22
8	200	31.75	31.73	31.89
9	207	26.96	27.01	27.17
10	215	23.87	23.72	23.88

Peak Signal to Noise ratio (PSNR) or the proportion of Maximum Power to Noise Power[29], is a decibel-based metric that can be used to assess the quality of a reconstructed image. The PSNR measured for all bands and few selected bands of PSNRs are mentioned in the Table 1 .

When compared to the CP decomposition method after Salinas HS image reconstruction, Tucker decomposition approaches offer good quality.HOSVD Tucker gives somewhat better results than ALS Tucker.The time taken to compress the tensor into core and component matrices is more for CP decompositions method and less for HOSVD Tucker decompositions as shown in Fig 9 and HOSVD tucker takes less time to recreation of Salinas HS image compared to other two methods as shown in Fig 10.

S.No	BANDS	CP	TD_ALS	TD_HOSVD
1	7	37.88	38.29	38.37
2	28	42.41	43.85	44.05
3	42	41.31	44.73	44.88
4	60	32.03	34.2	34.43
5	98	35.71	35.64	35.73
6	125	33.58	33.91	33.99
7	150	25.65	24.10	24.20
8	174	26.21	24.57	24.63
9	180	22.49	23.01	23.08
10	195	17.84	17.97	18.12

Table 2 : PSNRs of Indian Pines corrected HS image

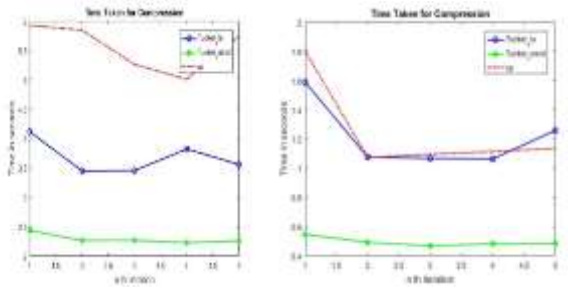

Fig 9 : Time taken to compress for Salinas and Indian Pine HS Image Data set

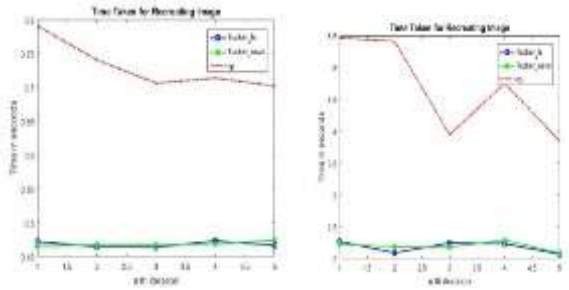

Fig 10 : Time taken to reconstruct the Salinas and Indian Pine HS Image Data set

Structural Similarity index (SSIM) [30] is an image fidelity metric that has proven to be quite successful in determining signal fidelity. The SSIM metric is a perceptual metric that classifies picture quality decline due to processing. In reality, it assesses the perceptual disparity between the reconstructed and original HS images.When utilizing SSIM, the HOSVD Tucker technique outperforms other decompositions in terms of perception image quality as shown in Table 2. The fundamental idea is to compress a given HS image by transforming it to a tensor using tensor decomposition algorithms.Table 3 shows that the HOSVD Tucker decomposition method compresses Salinas HS image data more than the CP and ALS Tucker decomposition methods.

The same procedure is repeated for Indian pines corrected HS image data set. Performance factors PSNR, SSIMof HOSVD are better than other two methods as shown in Table 4. Time taken to compress and to recreate is less compared to CP and Tucker ALS methods for Indian pines corrected image also. Compared to CP decomposition and Tucker decomposition using the ALS approach, Tucker decomposition using HOSVD compresses more while preserving good perception quality.

Table 3: Conclusion Table of Salinas HS image

Parameters	CP	Tucker ALS	Tucker - HOSVD
PSNR (dB)	32.68	32.97	33.09
Average SSIM	0.82	0.61	0.82
Elapsed Time(s) for compression	5.54	3.41	2.17
Elapsed Time(s) for Decompression	4.69	2.38	2.27
CR	86.55	88.79	96.69

Table 4: Conclusion Table of Indian Pines HS image

Parameters	CP	Tucker ALS	Tucker - HOSVD
PSNR (dB)	32.344	33.807	33.949
Average SSIM	0.591	0.521	0.517
Elapsed Time(s) for compression	5.546	3.409	2.179
Elapsed Time(s) for Decompression	4.695	2.383	2.275
CR	301.299	449.44	483.85

V. CONCLUSION

In this paper, three effective tensor decompositions have been used to compress the hyper spectral image by representing it as a 3D tensor. A tensor decomposition method removes both spatial and spectral redundancy present in the hyper spectral image. Experimentation on two real data sets demonstrated that the Tucker decomposition using the HOSVD method outperforms in terms of PSNR and SSIM with high compression compared to the other two methods. For the Indian Pines data set, HOSVD outperforms the other two approaches by around 1 and 2 dB in terms of PSNR, and by 48 and 182 in terms of compression ratio. The ALS method is straightforward to comprehend and use, but it requires several iterations to converge, and convergence is not guaranteed. When compared to CP decomposition and Tucker decomposition-ALS, Tucker-HOSVD requires less time with excellent compression and decent image quality as it is a non-iterative approximation. In the future, we can explore additional non-iterative approximations for decompositions to reduce the time. In order to improve the performance in different applications, this work might be extended to additional issues like classification and unmixing.

REFERENCES

[1]. Park, B. & Lu, R.. (2015) "Hyper Spectral Imaging technology in Food and Agriculture". 10.1007/978-1-4939-2836-1.

[2]. Willoughby, C. T., Folkman, M. A., & Figueroa, M. A. (1996)" Three-Dimensional and Unconventional Imaging for Industrial Inspection and Metrology", SPIE Digital Library.

[3]. Saari, H., Aallos, V-V., Akujärvi, A., Antila, T., Holmlund, C., Kantojärvi, U., Mäkynen, J., &Ollila, J. (2009). Novel miniaturized hyperspectral sensor for UAV and space applications. In R. Meynart (Ed.), Sensors, Systems, and Next-Generation Satellites XIII [74741M-1] International Society for Optics and Photonics SPIE. Proceedings of SPIE No. 7474 https://doi.org/10.1117/12.830284

[4]. Z.Ting-ting, L. Fei, (2012)"Application of Hyper Spectral Remote sensing in mineral identification and mapping" Proceedings of 2012 2nd ICCSNT, pp. 103-106.

[5]. H.F. G and P. Geladi (2007)," Techniques and Applications of Hyper spectral Image Analysis, U.K., Wiley.

[6]. C.H,R.Z and T. Peng (2009),"Lossless compression of hyper spectral images based on searching optimal multi bands for prediction ",
IEEE Geosci, Remote Sens,Vol.6,no 2,pp 339-343.

[7]. Lorenz, S. et al.(2018)Radiometric correction and 3D integration of long-range ground-based hyperspectral imagery for mineral exploration of vertical outcrops. Remote Sens. 10, 176.

[8]. YamanDua, Vinod Kumar, Ravi Shankar Singh(2020) "Comprehensive review of hyperspectral image compression algorithms," Opt. Eng. 59(9) 090902.

[9]. Karami, et al(2010) "Hyper spectral image compression based on tucker decomposition and discrete cosine transform," in 2nd Int. Conf. Image Process. Theory, Tools and Appl., 122 –125.

[10]. Karami, M. Yazdi and G. Mercier,(2012) "Compression of Hyper Spectral images using Discrete Wavelet Transform and Tucker Decomposition," IEEE J. Sel. Top. Appl. Earth Obs. Remote Sens., 5 (2), 444 –45.

[11]. X. Wang et al. (2018)"Distributed source coding of Hyper Spectral images based on three-dimensional wavelet," J. Indian Soc. Remote Sens., 46 (4), 667 – 673.

[12]. Kai-jenCheng et al, (2013) Hyperspectral images lossless compression using the 3D binary EZW algorithm", Proc. SPIE 8655, Image Processing: Algorithms and Systems XI, 865515.

[13]. Karami, R. Heylen and P. Scheunders, (2016) "Hyper spectral image compression optimized for

spectral unmixing," IEEE Trans. Geosci. Remote Sens., 54 (10), 5884 –5894.
[14]. Wavelet Techniques(2017) International Journal of Recent Research Aspects ISSN: 2349- 7688, Vol. 4, Issue 2 2, pp. 37-40.
[15]. Yingyue Bi, Yingcong Lu, Zhen Long, Ce Zhu, YipengLiu, Chapter(2022) "Tensor decompositions: computations, applications, and challenges", YipengLiu ,Tensors for Data Processing, Academic Press.
[16]. Fang L, He N, Lin H,(2019)"CP tensor-based compression of Hyper Spectral images", J Opt Soc Am A Opt Image Sci Vis.1;34(2):252-258.
[17]. N. Renard and S. Bourennane (2009) "Dimensionality Reduction Based on Tensor Modeling for Classification Methods," in IEEE Transactions on Geoscience and Remote Sensing, vol. 47, no. 4, pp. 1123-1131.
[18]. M. A. Veganzones et al(2016) "Nonnegative Tensor CP Decomposition of Hyperspectral Data," in IEEE Transactions on Geoscience and Remote Sensing, vol. 54, no. 5, pp. 2577-2588.
[19]. M. Jouni, M. D. Mura and P. Comon,(2019) "Hyper spectral Image Classification Using Tensor CP Decomposition," IGARSS 2019 - 2019 IEEE International Geoscience and Remote Sensing Symposium, pp. 1164-1167.
[20]. Phan, A. Cichocki and P. Tichavský, "On Fast algorithms for orthogonal Tucker decomposition," 2014 IEEE International Conference on Acoustics, Speech and Signal Processing (ICASSP), 2014, pp. 6766-6770.
[21]. Lee, G. (2018)" Fast computation of the compressive hyper spectral imaging by using alternating least squares methods", Signal Processing: Image Communication, 60, 100–106. .
[22]. Wang, L., Bai, J., Wu, J., & Jeon, G. (2015) "Hyperspectral image compression based on lapped transform and Tucker decomposition", Signal Processing: Image Communication, 36, 63– 69.
[23]. Kolda, Tamara G. and Brett W. Bader.(2009) "Tensor Decompositions and Applications" SIAM Rev. 51 455-500.
[24]. Hitchcock, F. L. (1927)"The Expression of a Tensor or a Polyadic as a Sum of Products", Journal of Mathematics and Physics, 6(1-4), 164–189.
[25]. Hitchcock, F. L. (1928)" Multiple Invariants and Generalized Rank of a P-Way Matrix or Tensor", Journal of Mathematics and Physics, 7(1-4), 39–79.
[26]. Carroll, J.D., Chang, JJ.(1970)"Analysis of individual differences in multidimensional scaling via an n-way generalization of "Eckart-Young" decomposition", Psychometrika 35, 283–319
[27]. Harshman, Richard A.(1970) "Foundations of the PARAFAC procedure: Models and conditions for an "explanatory" multi-model factor analysis"
[28]. Kiers, H. A. L. (2000)." Towards a standardized notation and terminology in multi way analysis. Journal of Chemometrics, 14(3), 105–122.
[29]. Neto, Arthur &Victorino, Alessandro &Fantoni, Isabelle & Zampieri, D. & Ferreira, Janito & Lima, Danilo,(2013) " Image Processing Using Pearson's Correlation Coefficient: Applications on Autonomous Robotics", Proceedings of the 2013 13th ICARS, ROBOTICA.
[30]. Ndajah, Peter & Kikuchi, Hisakazu & Yukawa, Masahiro & Watanabe, Hidenori &Muramatsu, Shogo(2010)" SSIM image quality metric for denoised images, ICVIS - Proceedings. 53-57.

B. Sucharitha received her M.Tech degree in Systems and Signal Processing from Jawaharlal Nehru Technological University, Hyderabad, India in 2013. She is currently working toward her Ph.D. degree in image processing at Jawaharlal Nehru Technological University, Hyderabad, India. Her primary research interests include image and video processing, compression, classification, remote sensing 3D imaging and optimization techniques.

Dr.AnithaSheela Kancharla received her Ph.D. degree from Jawaharlal Nehru Technological University, Hyderabad, India in the year of 2008. She is currently a Professor in the Electronics and Communication Department at Jawaharlal Nehru Technological University in Hyderabad, India. She conducted and published several papers in the areas of speech, audio, image and video signal processing, neural networks, signal processing and analog & digital communications.